ELSEVIER

Quaternary Science Reviews 25 (2006) 3216–3227

QSR

Marine-derived ^{14}C calibration and activity record for the past 50,000 years updated from the Cariaco Basin

K. Hughen[a,*], J. Southon[b], S. Lehman[c], C. Bertrand[a], J. Turnbull[c]

[a]*Department of Marine Chemistry and Geochemistry, Woods Hole Oceanographic Institution (WHOI), Woods Hole, MA 02543, USA*
[b]*Department of Earth System Science, University of California, Irvine, CA 92697, USA*
[c]*Institute of Arctic and Alpine Research, University of Colorado, Boulder, CO 80309, USA*

Received 27 November 2005; accepted 1 March 2006

Abstract

An expanded Cariaco Basin ^{14}C chronology is tied to ^{230}Th-dated Hulu Cave speleothem records in order to provide detailed marine-based ^{14}C calibration for the past 50,000 years. The revised, high-resolution Cariaco ^{14}C calibration record agrees well with data from ^{230}Th-dated fossil corals back to 33 ka, with continued agreement despite increased scatter back to 50 ka, suggesting that the record provides accurate calibration back to the limits of radiocarbon dating. The calibration data document highly elevated $\Delta^{14}C$ during the Glacial period. Carbon cycle box model simulations show that the majority of observed $\Delta^{14}C$ change can be explained by increased ^{14}C production. However, from 45 to 15 ka, $\Delta^{14}C$ remains anomalously high, indicating that the distribution of radiocarbon between surface and deep ocean reservoirs was different than it is today. Additional observations of the magnitude, spatial extent and timing of deep ocean $\Delta^{14}C$ shifts are critical for a complete understanding of observed Glacial $\Delta^{14}C$ variability.

1. Introduction

Calibration of the last 26 ka of the ^{14}C timescale has recently been advanced with the publication of the IntCal04 data set (Reimer et al., 2004). The new results rely on tree rings to provide bi-decadal resolution from 0 to 12,400 calendar years before present (0–12.4 ka) and are extended with comparable resolution to about 14.7 ka using varved marine sediments from the Cariaco Basin and ^{230}Th-dated fossil corals. From 14.7 to 26 ka, coral data alone control the IntCal04 curve, but at lower (approximately centennial) resolution. Beyond 26 ka, a comparison of data sets from previous studies showed considerable scatter and no single ^{14}C calibration curve was constructed for this interval (van der Plicht et al., 2004). More recently, an extensive array of ^{14}C and ^{230}Th-dated coral results have been presented, providing marine-based calibration with irregular sample spacing back to 50 ka (Fairbanks et al., 2005).

Here we present an updated marine-derived ^{14}C calibration from Cariaco Basin sediments for the last 50 ka (Hughen et al., 2004a) based on a revised calendar age model and additional ^{14}C measurements (increasing both the ^{14}C sampling resolution and the number of replicates). Cariaco Basin sediments are only intermittently laminated beyond ~14.7 ka, but show distinct millennial-scale variability in sedimentological and geochemical records that can be reliably correlated with Dansgaard–Oeschger (D–O) events in Greenland ice cores (Peterson et al., 2000). In previous work, Hughen et al. (2004a) exploited this relationship in order to map the GISP2 Greenland ice core layer count chronology of Meese et al. (1997) onto the Cariaco Basin ^{14}C series. However, GISP2 age uncertainties increase dramatically prior to 40 ka and, as noted by Southon (2004), significant differences between the GISP2 and GRIPsea (Johnsen et al., 2001) ice core chronologies remain unresolved. These discrepancies have led us to seek an alternative calendar age model based on absolute radiometric ages. Here we correlate high-resolution paleoclimate records from Cariaco Basin sediments (gray scale, 550 nm reflectance) and ^{230}Th-dated Hulu Cave speleothems ($\delta^{18}O$) in order to transfer the ^{230}Th Hulu Cave

*Corresponding author. Tel.: +1 508 289 3353; fax: +1 508 457 2193.
E-mail address: khughen@whoi.edu (K. Hughen).

0277-3791/$ - see front matter © 2006 Elsevier Ltd. All rights reserved.
doi:10.1016/j.quascirev.2006.03.014

chronology of Wang et al. (2001) onto the updated Cariaco ^{14}C series. Where Cariaco Basin and coral data sets overlap they appear to agree well, suggesting that the higher resolution of the ^{14}C dating in the Cariaco Basin can be used to accurately interpolate the calibration between lower resolution coral data.

2. Background

2.1. Cariaco Basin

The Cariaco Basin is located off the coast of Venezuela at the northern limit of seasonal migration of the Intertropical Convergence Zone (ITCZ). Updated calibration results come from ODP Leg 165 Site 1002 (Hughen et al., 2004a), which was drilled close to the site of piston core PL07-58PC used for high-resolution ^{14}C calibration during the last deglaciation (Hughen et al., 2000). The sites share the same hydrographic and climatic regimes, and sediments can be correlated between piston cores and ODP holes with great precision based on visual marker horizons and geophysical data (magnetic susceptibility, GRAPE density). The climatology and sedimentology of the Cariaco Basin have been described in detail elsewhere (Hughen et al., 2000; Peterson et al., 2000) and demonstrate synchronous deglacial changes in Cariaco and Greenland records, consistent with southward shifts in the ITCZ during cold (stadial) climates in the North Atlantic region (Rind et al., 1986, 2001; Schiller et al., 1997; Chiang and Bitz, 2005).

Evidence that the local Cariaco Basin reservoir age has varied little, even during stadial conditions, is provided by agreement between Cariaco and German pine ^{14}C dates during the last deglaciation and early Holocene, including the rapid shift from intense to reduced upwelling at the Younger Dryas/Preboreal transition (Hughen et al., 2000). In contrast, a floating tree ring chronology and ^{14}C record that has been tentatively anchored to Cariaco data suggests that the reservoir age may have changed during the Allerod or transition into the early Younger Dryas (Kromer et al., 2004). However, there are at least two plausible placements of the floating tree ring chronology against Cariaco records (e.g., Friedrich et al., 2001) and they must be considered preliminary until an anchored tree ring chronology is established.

2.2. Climatological linkages

Independent calendar-age chronologies for high-resolution paleoclimate records during the last deglaciation show that abrupt changes in the Cariaco Basin, Hulu Cave and Greenland were synchronous, within dating uncertainties (Hughen et al., 2000; Wang et al., 2001). (Paleoclimate records from speleothems dated by U-series showed age differences of up to 2–3 ka (Wang et al., 2001; Spotl and Mangini, 2002; Burns et al., 2003), but measurement errors were later identified that accounted for most of this discrepancy (Burns, 2004)). The implied synchroneity is consistent with studies that identified abrupt climate shifts in proxies for high and low latitudes from the same archive, and found no significant stratigraphic lag between tropical and high-latitude shifts (Severinghaus et al., 1998; Severinghaus and Brook, 1999; Hughen et al., 2004b). Here we assume that the temporal linkage demonstrated for deglacial changes was also valid during the previous Glacial interval, and specifically that Cariaco and Hulu Cave paleoclimate records show synchronous changes throughout their lengths.

3. Methods

3.1. ^{14}C Chronology

To the 280 ^{14}C dates previously presented by Hughen et al. (2004a) 187 new ^{14}C dates have been added. For the new as well as previous dates, samples of *Globigerina bulloides* or *Globigerinoides ruber* (typically 700–2000 foram tests, about 1 mg of carbon) were picked from the $>250\,\mu m$ sediment fraction after wet sieving. Measurements were performed on monospecific samples whenever possible, although mixed species assemblages were used for 25 samples with low overall foraminiferal abundance. Interspecies comparisons show no discernable offset in ^{14}C age. Samples were cleaned by sonicating in methanol and were leached with 0.001 N HCl prior to hydrolysis with H_3PO_4. The evolved CO_2 was purified cryogenically and converted to graphite in laboratories at Lawrence Livermore (CAMS-LLNL), University of Colorado (NSRL) and University of California at Irvine (UCI) using hydrogen reduction with an iron catalyst. Radiocarbon was measured by AMS at CAMS-LLNL, UCI, and Woods Hole Oceanographic Institution (NOSAMS).

Results are expressed as conventional radiocarbon ages, $\Delta^{14}C$ and Fm (Fraction modern) (Stuiver and Polach, 1977). The 1-sigma uncertainties quoted include contributions from measurements of blanks and normalizing standards, and are based on the scatter in data from multiple determinations during a 12–24 h measurement run as well as propagation of counting uncertainties. Results are presented as finite radiocarbon ages whenever the background-subtracted radiocarbon Fm values are more than two standard deviations from zero (Stuiver and Polach, 1977). The resulting finite age limits depend almost exclusively on the background scatter, since AMS readily allows even samples as old as 55–60 ^{14}C ka to be measured to statistical precisions of a few percent.

Backgrounds were determined from results on mg-sized carbon blanks prepared from calcite and measured with each batch of unknowns. CAMS-LLNL blanks for ODP 1002 measurement runs during 1999 averaged $Fm = 0.00150 \pm 0.00046$ or 52 ± 2.5 ^{14}C ka ($n = 15$), and were marginally lower at $Fm = 0.00113 \pm 0.00031$ or 54 ± 2.2 ^{14}C ka ($n = 12$) for runs in 2000–2001 when data for core sections older than 45 cal ka were measured. NSRL/

NOSAMS blanks for ODP runs in 2000–2002 averaged Fm = 0.00150 ± 0.00048 or 52 ± 2.6 ^{14}C ka ($n = 20$). UC Irvine ODP blanks were Fm = 0.00174 ± 0.00043 or 51 ± 2.0 ^{14}C ka ($n = 8$) for 2003 and Fm = 0.00102 ± 0.00030 or 55 ± 2.3 ^{14}C ka ($n = 33$) for samples run in 2004–2005, including one batch graphitized at NSRL. The 25–35% uncertainties quoted above represent the long-term 1-sigma scatter in the backgrounds, but differences between results on replicate independent calcite aliquots from the same run were typically only ±20%, suggesting that real run-to-run blank variations were present for each of the sample preparation laboratories. Therefore, the blank for each set of unknowns was taken as the mean of the calcite results for that run, and uncertainties of ±20% were assigned for the blank corrections. Results from small calcite aliquots were used to determine size-dependent blanks for small samples (0.3–0.7 mg of carbon) picked from a few sections of the cores where foraminifera were

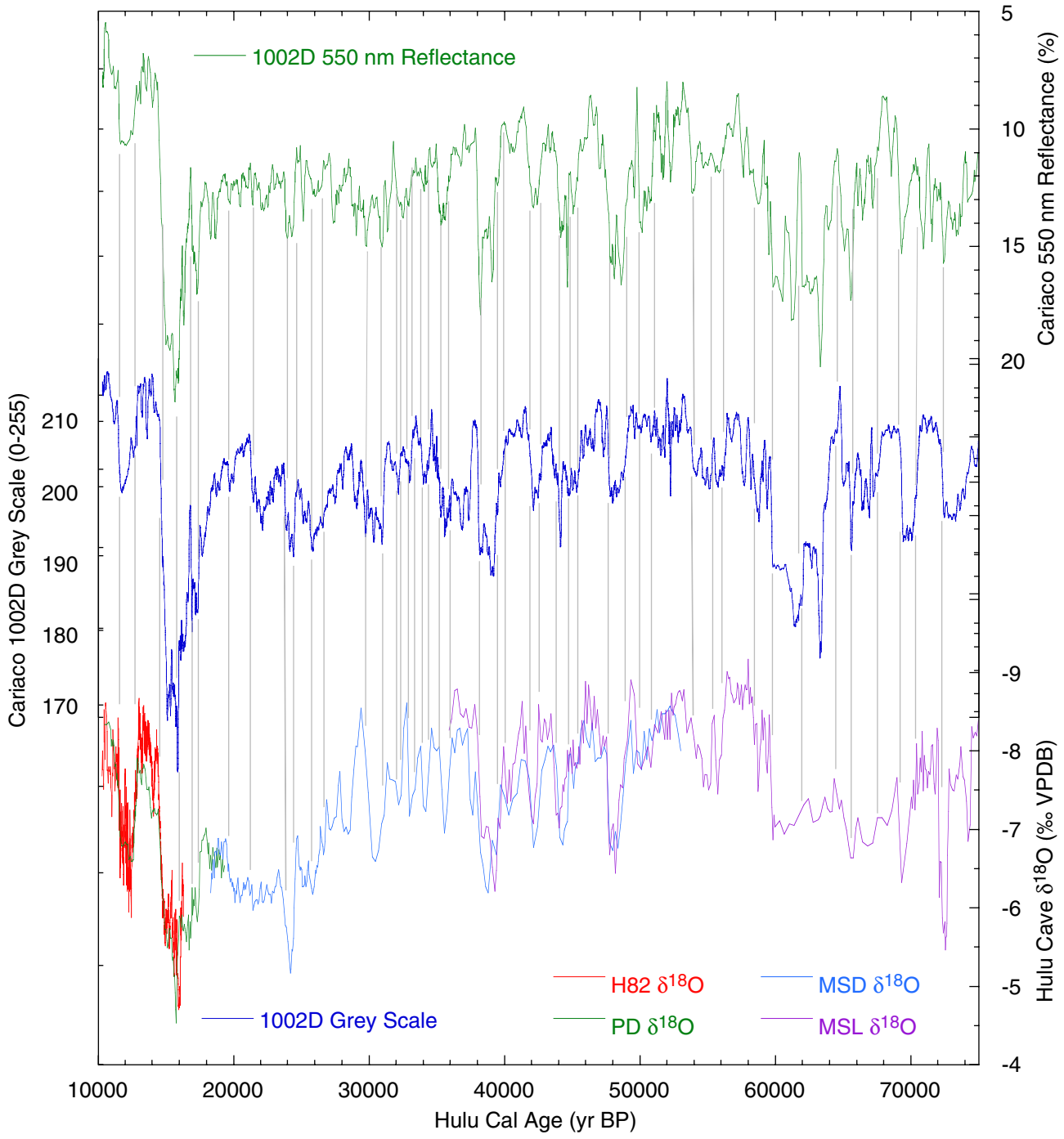

Fig. 1. High-resolution paleoclimate time series for Cariaco Basin sediment 550 nm and gray scale reflectance (top, middle) and Hulu Cave speleothem δ^{18}O (bottom), plotted against Hulu ^{230}Th calendar age. Tie lines used for correlating and aligning the Cariaco records to Hulu calendar age are shown in gray.

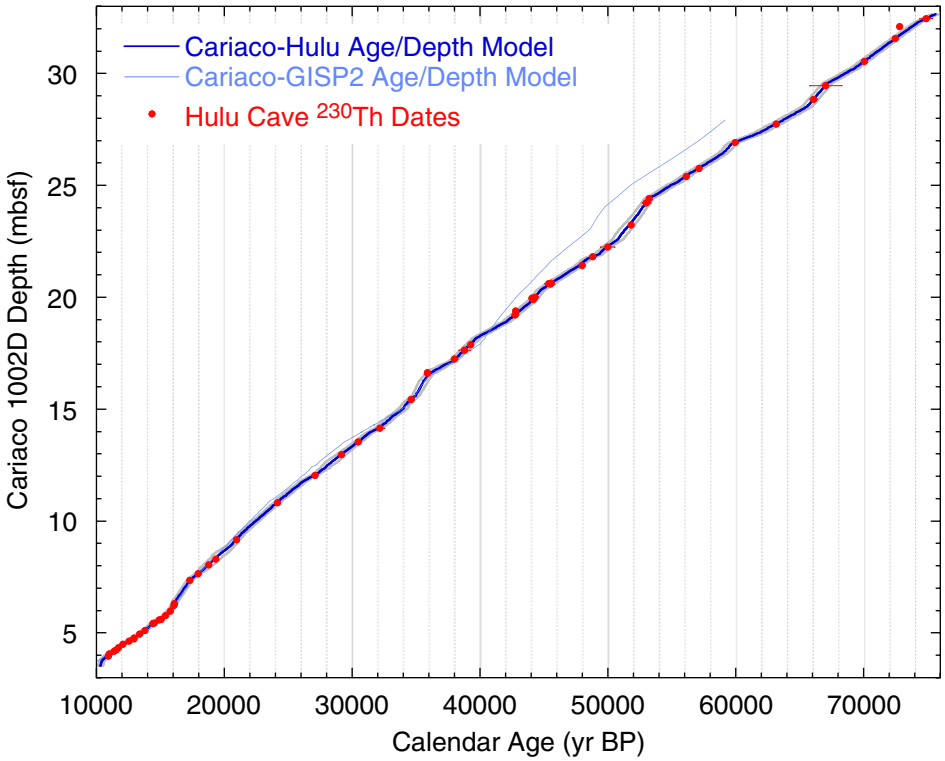

Fig. 2. Age-depth model for Cariaco Basin sediments tied to Hulu Cave ^{230}Th chronology (dark blue line, red circles). The previous age-depth model based on Cariaco correlation to GISP2 is shown in light blue. Both curves have been corrected to account for missing sediment around 14 mbsf due to a core break in Hole 1002D. Gray lines show the total 1-sigma calendar age uncertainty envelope for the Cariaco-Hulu chronology. Cariaco calendar age uncertainties are larger than the sample-to-sample resolution of the stratigraphically continous record and thus can not be plotted as error bars on individual points. Rather the whole curve can shift together within the bounds of the gray curves. Independent sample-to-sample calendar age uncertainties are constrained by plausible changes in sedimentation rate and scale as a function of depth interval between samples (considered negligible—not shown).

scarce. Uncertainties of $\pm 30\%$ were assigned, based on the long-term blank scatter. Agreement between data measured at our different laboratories, plus results from duplicate samples from the oldest part of the record, suggest that the background subtraction procedures are robust.

^{14}C and magnetic susceptibility measurements on Hole 1002D sediments showed disturbances every 10 m, coincident with the ends of successive core drives, and data obtained from these sections were removed from the records. Undisturbed samples were obtained from adjacent Hole 1002E, drilled in offsetting fashion, in order to construct a continuous record. Results were scrutinized closely if they came from small samples (<0.7 mg C), or from a single wheel containing targets that packed poorly at NSRL and which consequently did not perform well in the NOSAMS source. Results from these populations were removed ($n = 19$) if they differed by more than four sigma calculated from either replicates or immediately adjacent bracketing samples (see Table 1 caption). Thirteen additional samples were removed due to offsets of more than four sigma from surrounding samples. Records of ^{14}C and Δ^{14}C were constructed by removal of outliers as explained above, and averaging all duplicate (160), triplicate (60) and quadruplicate (8) measurements. The original data as well as averaged records are provided as Supplementary material in the online version (Table 1).

3.2. Calendar age model

The Hulu Cave chronology is based on 59 ^{230}Th dates from five individual stalagmites (Wang et al., 2001). Two of the stalagmites, YT and H82, also have internal chronologies based on annual banding in addition to ^{230}Th ages. The dates have 1-sigma uncertainties ranging from ± 50 years at 10 ka to ± 50 years at 50 ka. Where they overlap, the different stalagmite δ^{18}O records are virtually identical in their patterns and timing of abrupt changes. There is continuous growth in at least one stalagmite over the entire interval, providing an unbroken δ^{18}O record from 10 to 70 ka. The sampling resolution for ^{230}Th dating is ~400 years from 10 to 17 ka, ~1000 years from 17 to 20 ka, and ~1600 years from 20 to 60 ka for the stratigraphically continuous δ^{18}O record.

The Hulu Cave ^{230}Th age model was mapped onto the Cariaco Basin ^{14}C series by correlation of associated δ^{18}O and gray scale variations that define stadial and interstadial transitions using 46 tie points (Fig. 1). The resultant correlation is strong, $r = 0.6$. Because the Cariaco tie points correspond with abrupt climate transitions they tend

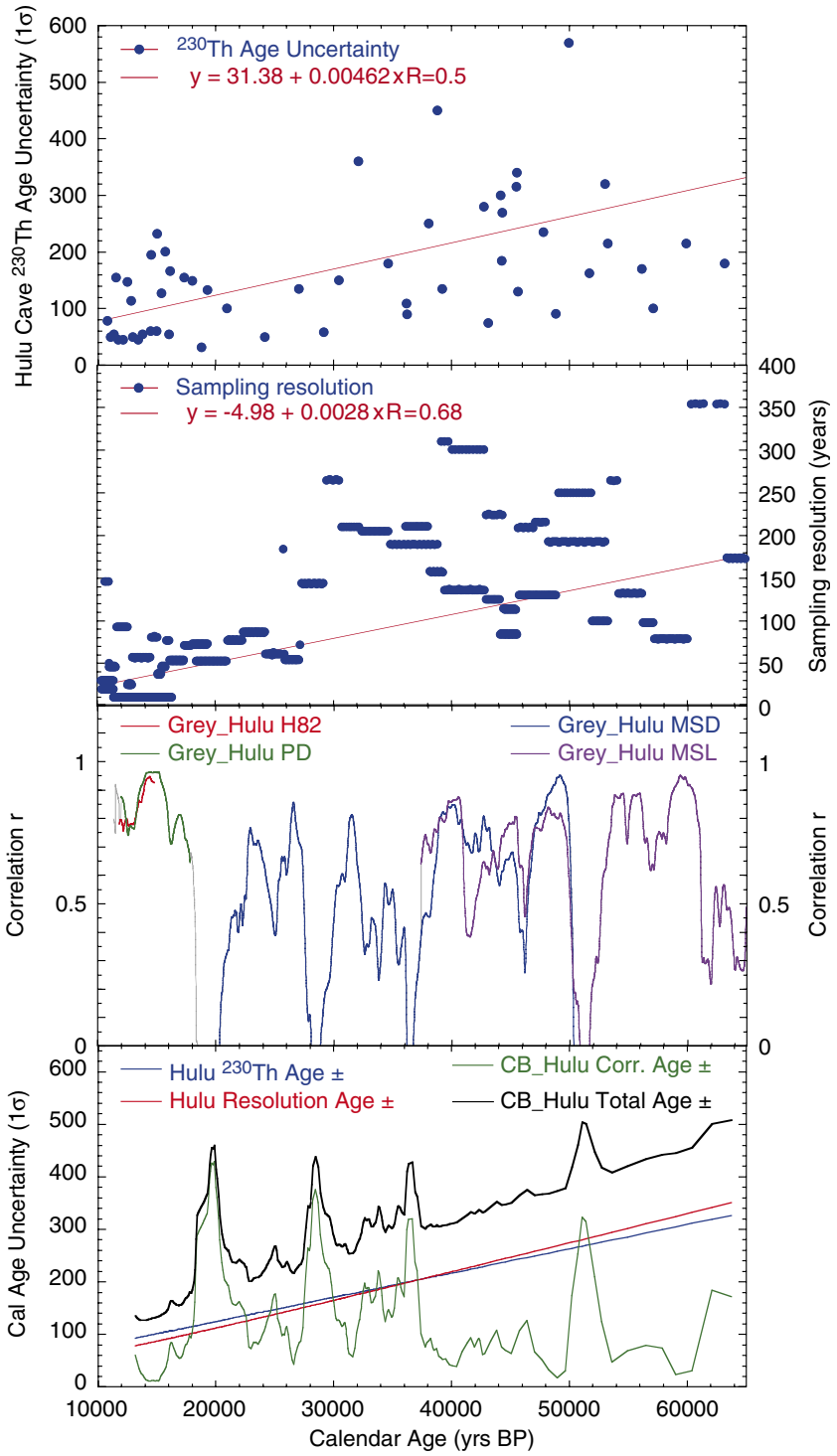

Fig. 3. (A) Hulu Cave ^{230}Th date uncertainties (1 σ) plotted versus ^{230}Th age. A linear fit to the data was used to calculate the contribution of Hulu ^{230}Th analytical errors to calendar age uncertainty in the Cariaco-Hulu age-depth model. (B) Hulu Cave speleothem δ^{18}O sampling resolution plotted versus ^{230}Th age. A linear fit to the data was used to calculate the contribution of Hulu Cave δ^{18}O sampling resolution to calendar age uncertainty in the Cariaco-Hulu age-depth model. (C) Plot of moving correlation between Cariaco gray scale and individual Hulu δ^{18}O records. Bold lines show results for a 3000-yr moving window, thin lines are for a 2000-yr window. Intervals of weak correlation are found centered around ~19, ~28, ~37 and ~51 ka. The strongest correlation for a given interval was scaled to provide a calendar age error term linked to the strength of correlation. In the lack of any correlation ($r \leqslant 0$) to Hulu Cave, we constrain Cariaco calendar age uncertainty by assuming that Cariaco sedimentation rate varies within a factor of two. The correlation r data were therefore scaled from a minimum 0 years (for perfect correlation $r = 1$) to a maximum 439 years ($r = -0.5$) to create an additional term for error as a function of correlation strength. D) The three sources of calendar age uncertainty plotted individually for comparison and combined in quadrature to provide the total calendar age uncertainty in years (1 sigma).

to bracket laminated (interstadial) versus massive (stadial) intervals with differing sedimentation rates (as previously noted by Peterson et al. (2000)). The calendar age-depth model for the Cariaco sediment record derived in this way is shown in Fig. 2 along with the previous age-depth model of Peterson et al. (2000) that was utilized in the original calibration (Hughen et al., 2004a). We also note that the original calendar age chronology for the interval from ~18 to 14.7 ka has been called into question. However, as shown in Fig. 1, the chronology within this interval is now well constrained by abrupt and well-correlated climate signals in the two archives.

There are three distinct sources of uncertainty affecting the derived calendar age model; the analytical uncertainty of the Hulu calcite ^{230}Th dating, the precision of correlation as limited by precision and resolution of the individual time series, and the accuracy of the cross-correlation procedure. One-sigma uncertainties reported for the 59 ^{230}Th dates show an increasing trend with age (Fig. 3a). Their contribution to the total calendar age uncertainty was estimated by simple linear regression. The precision of cross correlation includes sources of potential error that are independent of the correlation itself (i.e., assuming a perfect correlation coefficient). For example, where individual Hulu Cave δ^{18}O records overlap they show slightly different ages for abrupt changes (well within analytical uncertainties). The average age difference for all overlapping events is 90 years, representing a constant source of $\pm$45 year uncertainty. In addition, we conservatively assume that the precision of the cross-correlation also varies as twice the resolution of the limiting (lower) resolution record. The sampling resolution for all five Hulu Cave stalagmites shows an increasing trend with age (Fig. 3b), and was fit with a linear curve. This term was added in quadrature with the Hulu age-difference term above to calculate the uncertainty due to precision of the correlation. Finally, we consider the accuracy of the correlation itself in contributing to uncertainty. Moving cross-correlations with windows of 2000 and 3000 years were used to identify intervals of strong and weak correlation between gray scale and each δ^{18}O record (Fig. 3c). In general, the correlations are strong ($r > 0.5$), but several brief (1–2 kyr) intervals showing no correlation are centered at 19, 28, 37 and 51 ka. An estimated factor of two change in sedimentation rate was used to constrain relative age uncertainty within the longest Cariaco interval showing no

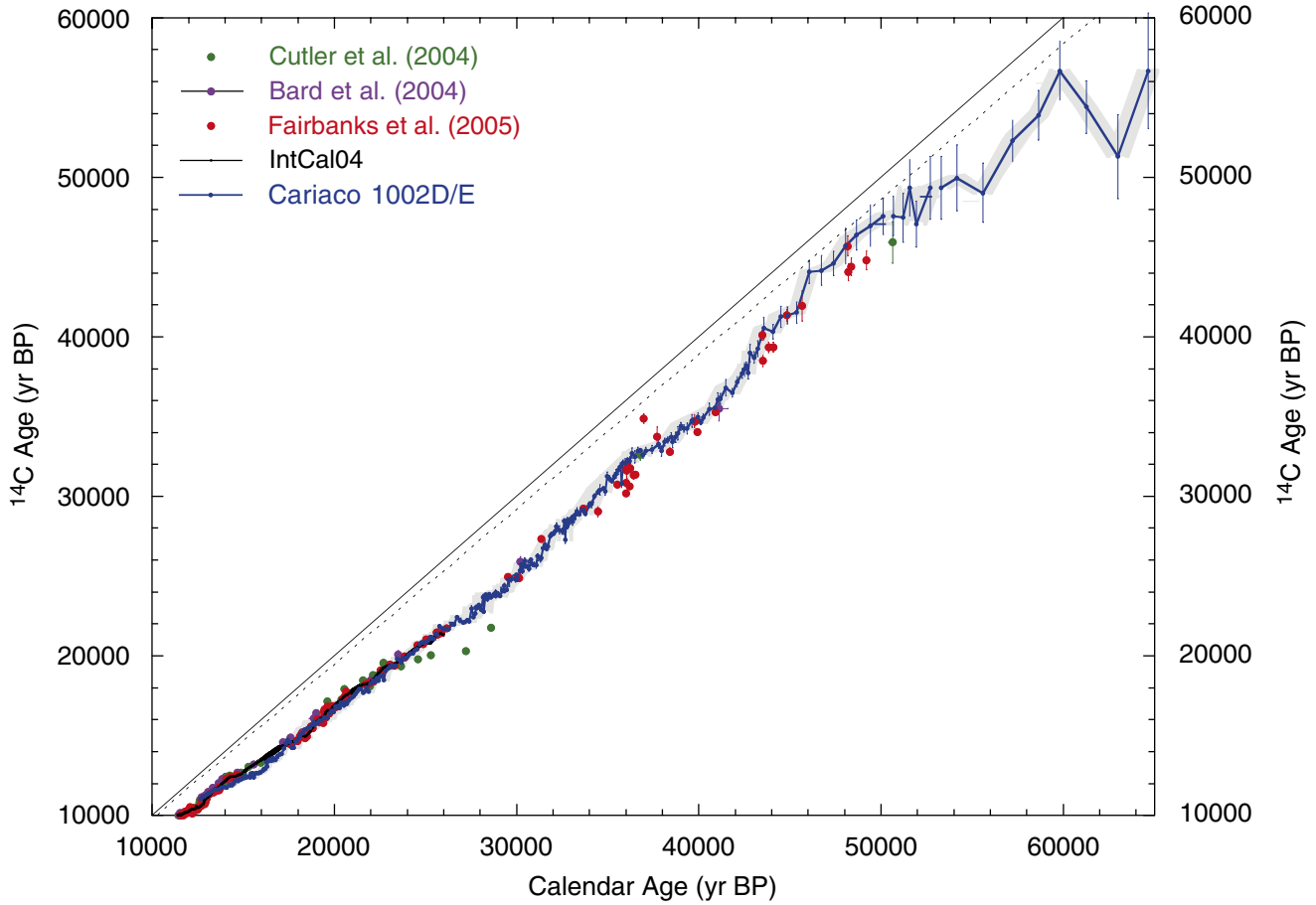

Fig. 4. Cariaco Basin ^{14}C ages plotted versus Hulu Cave calendar age model. High-resolution ^{14}C calibration data from IntCal04 are shown as a black line. Paired ^{230}Th/^{14}C dates from corals are shown as solid circles. All error bars are 1 sigma, and gray swath shows 1-sigma error envelope for Cariaco record due to calendar age uncertainty. The 1:1 age lines are shown based on Libby (1955) and consensus (Godwin, 1962) ^{14}C half-live values, 5568 years (solid line) and 5730 years (dotted line), respectively.

correlation to Hulu $\delta^{18}O$, providing a maximum uncertainty of ± 439 years. The moving correlation plot was then scaled between this maximum age uncertainty for correlation $r \leqslant 0$ and zero age uncertainty for a perfect correlation $r = 1$. The three separate sources of uncertainty were then summed in quadrature to provide total calendar age uncertainty for the Cariaco-Hulu age model (Fig. 3d).

4. Results

4.1. ^{14}C Records

The Cariaco ^{14}C series presented with respect to the Hulu Cave ^{230}Th chronology provides an updated marine-derived ^{14}C calibration for the past 50 ka (Fig. 4). The 1-sigma ^{14}C dating uncertainties are plotted as independent error bars. However, total calendar age uncertainties are larger than the sampling intervals of the stratigraphically continuous Cariaco record and are therefore not independent from point-to-point. Calendar age uncertainties are shown as an error envelope derived from the Hulu-Cariaco correlation procedure as above, within which the curve can shift (gray swath in Fig. 4). The calendar age errors for the Cariaco-Hulu age model, particularly older than 40 ka, are substantially smaller than before due to the larger uncertainty of the GISP2 chronology used earlier. As expected, the greatest departures from the original calibration data set are in the interval older than 40 ka, where the GISP2 chronology is least reliable. However, smaller but still significant differences are also present for the 21–33 ka interval. Most importantly, the upward revision of the calendar age flattens the calibration beyond 40 ka, maintaining it well below the "1:1" calendar vs. ^{14}C age line (Fig. 4). The Cariaco data are in good agreement with the coral data and IntCal04 curve from 10 to 33 ka. Beyond 33 ka, the Cariaco data follow the trend of the majority of coral data, although showing a tendency toward younger calendar ages for the interval older than 33 ka (Fig. 4).

A reconstruction of initial atmospheric ^{14}C activity based on the marine-derived calibration for the last 60,000 years is given in Fig. 5 (expressed as $\Delta^{14}C$, or per mil deviations from the pre-anthropogenic atmosphere, following the convention of Stuiver and Polach, 1977). As in our previous reconstruction, $\Delta^{14}C$ shows elevated values during the Glacial period >15 ka, preceded by a broad minimum from 50 to 45 ka. There are three sharp increases

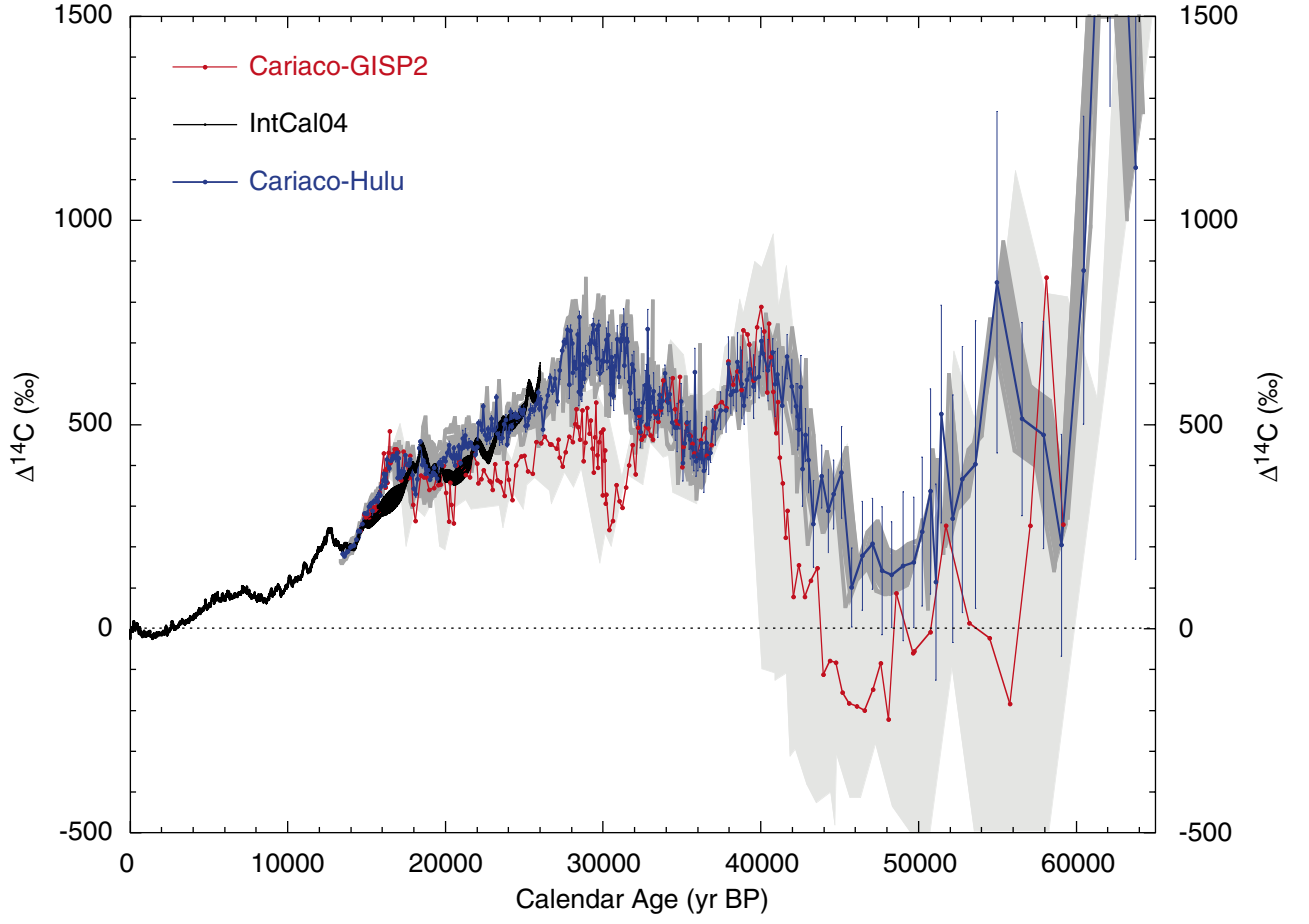

Fig. 5. Cariaco marine-derived ^{14}C activity ($\Delta^{14}C$) calculated with a constant reservoir correction of 420 years. The new Cariaco-Hulu record is plotted with the previous Cariaco-GISP2 $\Delta^{14}C$ record (Hughen et al., 2004a) for comparison. The error bars show $\Delta^{14}C$ uncertainty in the Cariaco-Hulu record due to 1-sigma errors in ^{14}C age measurement alone, whereas the dark and light gray swaths show the 1-sigma error envelopes for Cariaco versus Hulu Cave and GISP2, respectively, due to calendar age uncertainties alone.

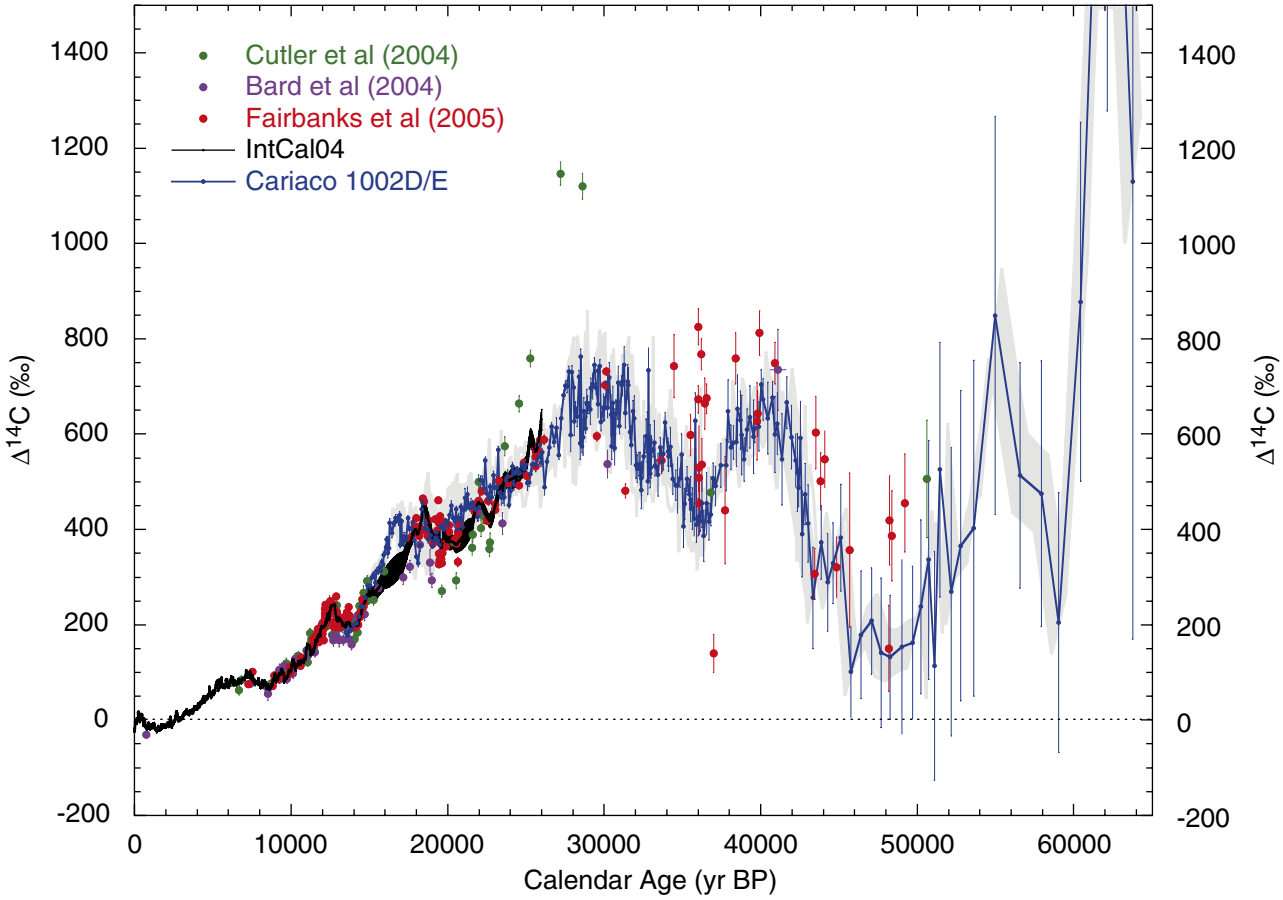

Fig. 6. Comparison of the updated Cariaco-Hulu $\Delta^{14}C$ record to $\Delta^{14}C$ from fossil corals, showing excellent agreement back to 33 cal ka ($r = 0.79$), and a continued strong correlation from 33 to 50 cal ka ($r = 0.58$), despite increased scatter. Error bars and symbols as in Fig. 5.

to local maxima centered around 40, 34 and 30 ka, and a smaller local maximum centered at 17 ka followed by a sharp decline. Most importantly, the flattening of the calibration relationship older than 40 ka described above produces significantly higher $\Delta^{14}C$ values before 40 ka than in the original reconstruction (Fig. 5). The large $\Delta^{14}C$ increase from 45 to 40 ka is also less abrupt and lower in amplitude than in the earlier reconstruction. The new Cariaco record shows excellent agreement with coral $\Delta^{14}C$ data from 10 to 33 ka ($r = 0.79$; Fig. 6) (Bard et al., 2004; Cutler et al., 2004; Fairbanks et al., 2005). There is also good agreement from 33 to 50 ka ($r = 0.58$), despite increasing temporal variability in each of the data sets. However, Cariaco $\Delta^{14}C$ values appear to be systematically lower than coral results in the older part of the record from 33 to 50 ka (Fig. 6). The $\Delta^{14}C$ offsets are too large to be explained by differences in reservoir age between sites, and may be due to slightly higher ^{230}Th calendar ages in the older corals than in the corresponding Hulu ^{230}Th chronology, although it is not yet possible to determine which of the chronologies is more reliable. Alternatively, the contamination problems that were encountered in the preparation of very old coral samples for radiocarbon measurements (e.g., Chiu et al., 2005) may have led to an underestimation of the true blank correction and a consequent biasing of the coral record to young ^{14}C ages.

5. Discussion

The new Cariaco-Hulu $\Delta^{14}C$ reconstruction confirms elevated values and large variability during the Glacial period and is in agreement with the majority of ^{230}Th-dated coral results back to 50 ka (Bard et al., 2004; Cutler et al., 2004; Fairbanks et al., 2005). Reconstructed activities during the Glacial period are in the range of 400–700‰, implying significantly greater ^{14}C production and possibly diminished uptake of ^{14}C by the ocean compared to the Holocene. In order to investigate the implications of the observed $\Delta^{14}C$ record, we used the carbon cycle box model of Hughen et al. (2004a). For these simulations, the model included an atmosphere, terrestrial biosphere, and surface and deep ocean reservoirs. ^{14}C production rates were calculated as a function of geomagnetic field intensity (Laj et al., 2002), according to Masarik and Beer (1999). For each experiment, the model was equilibrated with ^{14}C production rates at 60 ka, then a transient run was forced with changing production as above from 60 ka to the present. A constant scaling factor

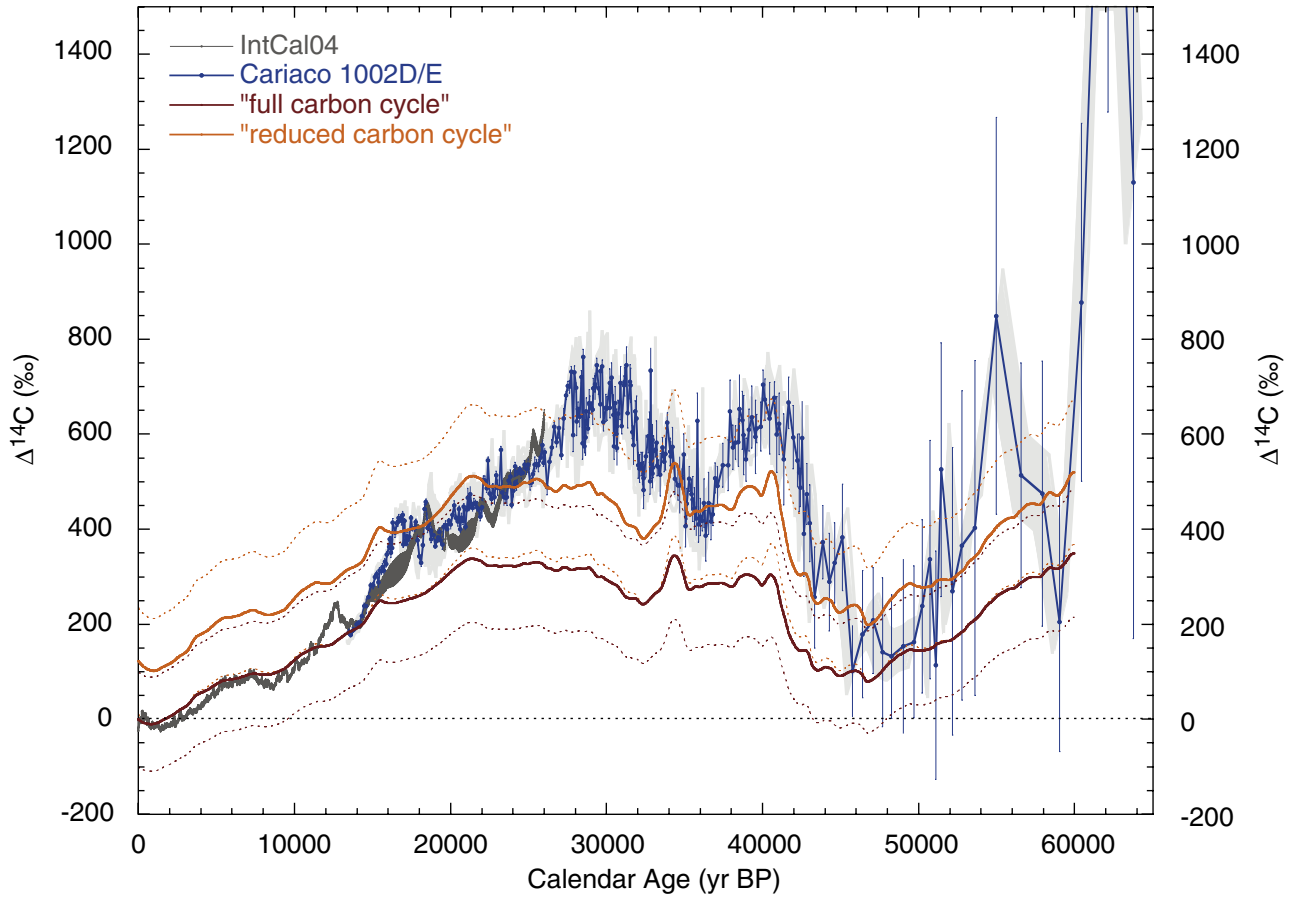

Fig. 7. Comparison of paleo-$\Delta^{14}C$ observations to $\Delta^{14}C$ simulated by a carbon cycle box model. The "full carbon cycle" represents preindustrial Holocene boundary conditions, whereas the "reduced carbon cycle" includes a 50% reduction in exchange between Surface Ocean and Deep Ocean reservoirs (as well as decreased C reservoirs in the atmosphere and terrestrial biosphere). ^{14}C production rate uncertainties are assumed to be $\pm 10\%$, and resulting $\Delta^{14}C$ uncertainties for both simulations are shown by dotted lines. The agreement between observed and modeled $\Delta^{14}C$ is much better than previously (Hughen et al., 2004a), particularly for ages >40 ka. Significant disagreement persists however, during intervals of observed high $\Delta^{14}C$. Error bars and symbols as in Figs. 5 and 6.

was applied to the production rates in order to tune the model reservoir $\Delta^{14}C$ values at model year 0 ka to observed modern values. For the pre-anthropogenic simulation ("full carbon cycle"), scaling production by -21% resulted in 0 ka reservoir $\Delta^{14}C$ values (Atmosphere 0‰, Terrestrial Biosphere -5‰, Surface Ocean -53‰, Deep Ocean -159‰) in good agreement with modern observations (Broecker and Peng, 1982, 1987; Siegenthaler and Oeschger, 1987; Kump, 1991; Quay et al., 2003). In order to account for the combined uncertainty in reconstruction of past geomagnetic field strength and its influence on ^{14}C production, we apply a constant $\pm 10\%$ uncertainty to the production rate history, which translates to ± 100–150‰ in the modeled curves.

The simulations produce a temporal pattern of $\Delta^{14}C$ change arising from ^{14}C production rate alone that is similar to the data (Fig. 7), consistent with the expectation that geomagnetically modulated changes in ^{14}C production will dominate the ^{14}C inventory on the 10^4-year timescale (set by the ^{14}C mean lifetime). However, the simulation produces maximum $\Delta^{14}C$ of only $\sim 300‰ \pm 100‰$ for the interval 20–40 ka, whereas observed $\Delta^{14}C$ exceeds the simulated changes by up to several hundred per mil, most prominently prior to ~ 27 ka.

In this simple model, reducing the surface-to-deep ocean exchange by 50% ("reduced carbon cycle") produces an additional atmospheric and surface ocean $\Delta^{14}C$ response of ~ 200‰, encompassing most of the glacial age data (Fig. 7). According to the model, however, the prescribed change in surface-to-deep ocean exchange would produce a doubling of the surface-to-deep ocean $\Delta^{14}C$ difference. Broecker et al. (2004) point out the difficulty that such a large change in Glacial ocean chemistry has not been observed in the western Pacific. However, observations do show evidence of decreased Glacial $\Delta^{14}C$ in the deep western (Keigwin, 2004) and eastern North Atlantic (Skinner and Shackleton, 2004), deep eastern Pacific (Shackleton et al., 1988; L. Keigwin, pers. comm.), and southwest Pacific (Sikes et al., 2000). We also note that most of the paleo-ocean $\Delta^{14}C$ reconstructions correspond to the period around the Last Glacial Maximum (~ 21 ka BP), an interval when the simulated $\Delta^{14}C$ response to production rates changes alone

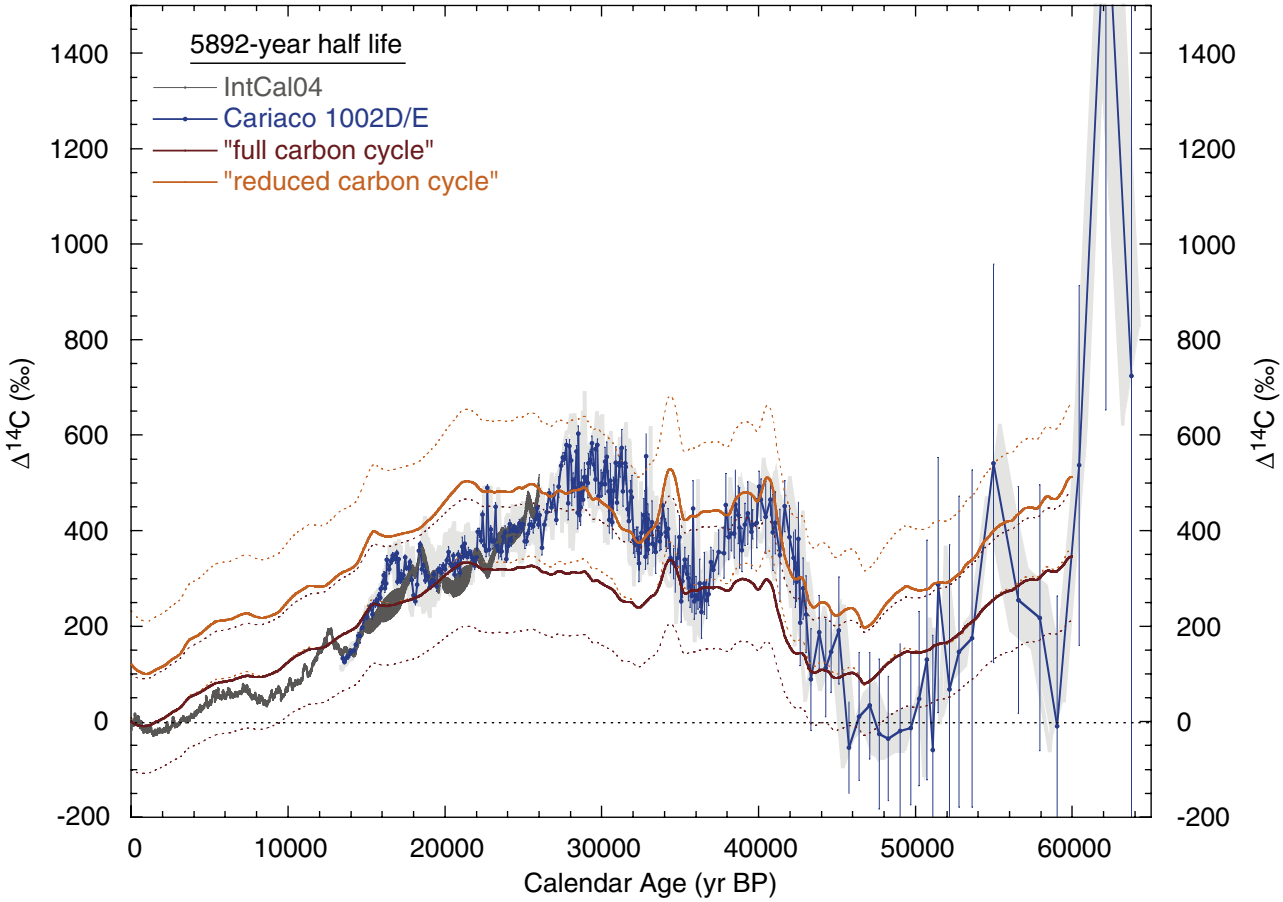

Fig. 8. Observed and simulated $\Delta^{14}C$ values calculated using a hypothetical ^{14}C decay constant 3% above the consensus value (hypothetical half-life of 5890 years). $\Delta^{14}C$ is reduced proportionally for older samples, and those with higher measured ^{14}C activity. Such an increase in ^{14}C half-life improves the comparison between observed and modeled $\Delta^{14}C$ during the earlier part of the record ~25–40 ka, but significantly decreases agreement during the Holocene. Error bars and symbols as in Figs. 5–7.

is close to the observations (especially if reasonable production rate uncertainties are considered) (Fig. 7). A more serious issue is that reconstructed rates of $\Delta^{14}C$ change at the beginning of the last deglaciation, ~17 ka, are too large to be explained by changes in production rate alone and require a substantial dilution of ^{14}C atoms in the atmosphere by a more depleted reservoir. Reconstructions of large transient changes during deglaciation in mid-to-intermediate depth $\Delta^{14}C$ of the western (Robinson et al., 2004) and deep eastern North Atlantic (Skinner and Shackleton, 2004) are consistent with a major reorganization of the ocean circulation and redistribution of ^{14}C, probably involving increased ventilation of a previously isolated (low $\Delta^{14}C$) deep water mass of southern or Pacific origin (e.g., Adkins et al., 2002; Sikes et al., 2000; Shackleton et al. 1988; L. Keigwin, pers. comm.).

Finally, the apparent difficulty of reconciling the $\Delta^{14}C$ reconstructions with plausible changes in ^{14}C production and distribution between global carbon reservoirs has led some investigators to suggest that the discrepancy may be due to uncertainty in the ^{14}C decay constant (Chiu et al., 2004) The current "consensus" half-life is 5730 years (Godwin, 1962), and is ~3% higher than the value originally reported by Libby (1955) (i.e., 5568 years). Applying a hypothetical half-life of 5890 years (an arbitrary 3% above the consensus value) for calculation of initial $\Delta^{14}C$ from the calibration data results in diminished Glacial values by as much as 200‰ (Fig. 8). The effect scales with both true age and measured ^{14}C activity, so the low values from 45 to 50 ka are not shifted as much as the surrounding high values.

Increasing the ^{14}C half-life by 3% also influences the model simulation of $\Delta^{14}C$. ^{14}C production rates must be reduced slightly more (by −23% instead of −21%) in order to tune the model reservoirs to the same observed $\Delta^{14}C$ values as above. With this adjustment, the "full" and "reduced" carbon cycle model simulations (Fig. 8) show only slightly higher $\Delta^{14}C$ than the previous results (e.g., Fig. 7). During the Glacial, modeled $\Delta^{14}C$ clearly lies in better agreement with observations. However, the agreement between simulated and observed $\Delta^{14}C$ change during the Holocene is now significantly worse (Fig. 8). The Holocene $\Delta^{14}C$ results based on tree ring measurements are not in question, suggesting that a simple correction to the ^{14}C half life is not the primary solution to the problem of elevated $\Delta^{14}C$ values during the Glacial period.

6. Conclusions

The new Cariaco Basin ^{14}C record linked to Hulu Cave radiometric ages provides an improved marine-based calibration data set for the past 50,000 years. The ^{14}C chronology shows less scatter than previously, due to the large numbers of replicate measurements and increased sample resolution. The calendar age model is based on ^{230}Th dates on clean speleothems, an almost ideal system for ^{230}Th dating. Calendar age errors due to dating uncertainties and correlation procedures are discussed in detail, and are generally smaller (and better defined) than those of the prior reconstruction based on correlation to GISP2, particularly in the interval older than 40 ka. The agreement between the updated Cariaco results and ^{230}Th-dated coral data is markedly improved for the 20–33 ka interval, and the data sets continue to show good agreement back to 50 ka. The convergence of independent calibration data from marine Cariaco Basin-Hulu Cave, fossil corals (Bard et al., 2004; Cutler et al., 2004; Fairbanks et al., 2005) and terrestrial speleothems (at least back to 33 ka; Beck et al., 2001) supports the accuracy of the records and suggests that reliable calibration is possible back to the limits of radiocarbon dating.

Our new record documents highly elevated $\Delta^{14}C$ values during the Glacial period, confirming previous observations. Carbon cycle box model simulations show that more than half of the observed $\Delta^{14}C$ change can be explained by increased cosmogenic production resulting from changes in Earth's geomagnetic field intensity. However, for portions of the record between 45 and 15 ka, observed $\Delta^{14}C$ lies well above modeled values, suggesting that fewer ^{14}C atoms entered deep ocean reservoirs due to reduced vertical mixing in the ocean relative to today. Additional data are needed to place constraints on the magnitude, spatial extent and timing of deep ocean $\Delta^{14}C$ anomalies for comparison to observations of surface ocean and atmospheric $\Delta^{14}C$.

Acknowledgements

This paper is dedicated to the memory of Professor Sir Nicholas J. Shackleton, who provided constant and valuable scientific feedback throughout the course of this research. In particular, KAH would like to acknowledge the valuable, long-standing guidance and mentorship he received from Shackleton starting at the very beginning of his career. This was a tremendous boost to a young scientist for which he is eternally grateful.

This work was supported by US NSF (OCE-0117356), Lawrence Livermore National Laboratory (LDRD-97-ERI-009), the US Department of Energy (W-7405-Eng-48) and the Dean of Science, UC Irvine. We thank the ODP Core Repository in Bremen for core sampling and staff of the UC Irvine, LLNL and NOSAMS AMS labs for sample preparation assistance.

Appendix A. Supplementary materials

The online version of this article contains additional supplementary data. Please visit doi:10.1016/j.quascirev.2006.03.014.

References

Adkins, J.F., McIntyre, K., Schrag, D.P., 2002. The salinity, temperature, and $\delta^{18}O$ of the glacial deep ocean. Science 298, 1769–1773.

Bard, E., Guillemette, M.-C., Frauke, R., 2004. Present status of radiocarbon calibration and comparison records based on Polynesian corals and Iberian margin sediments. Radiocarbon 46, 1189–1201.

Beck, J.W., Richards, D.A., Edwards, R.L., Silverman, B.W., Smart, P.L., Donahue, D.J., Hererra-Osterheld, S., Burr, G.S., Calsoyas, L., Jull, A.J.T., Biddulph, D., 2001. Extremely large variations of atmospheric ^{14}C concentration during the last Glacial period. Science 292, 2453–2458.

Broecker, W., Barker, S., Clark, E., Hajdas, I., Bonani, G., Lowell, S., 2004. Ventilation of the glacial deep Pacific Ocean. Science 306, 1169–1172.

Broecker, W.S., Peng, T.-H., 1982. Tracers in the Sea. LDGO, Palisades, NY, 690pp.

Broecker, W.S., Peng, T.-H., 1987. The oceanic salt pump: Does it contribute to the glacial-interglacial difference in atmospheric CO_2 content? Global Biogeochemical Cycles 1, 251–259.

Burns, S.J., 2004. Correction to "indian ocean climate and an absolute chronology over Dansgaard/Oeschger events 9 to 13. Science 301, 1365–1367 Science 305, 1565.

Burns, S.J., Fleitmann, D., Matter, A., Kramers, J., Al-Subbary, A.A., 2003. Indian ocean climate and an absolute chronology over Dansgaard/Oeschger events 9 to 13. Science 301, 1365–1367.

Chiang, J.C.H., Bitz, C.M., 2005. Influence of high latitude ice cover on the marine Intertropical Convergence Zone. Climate Dynamics.

Chiu, T., Fairbanks, R.G., Mortlock, R.A., 2004. Radiocarbon Calibration Between 30,000 and 50,000 Years Before Present Using Fossil Corals. EOS Trans. AGU 85(47), Fall Meet. Suppl., S.F., CA.

Chiu, T.-C., Fairbanks, R.G., Mortlock, R.A., Bloom, A.L., 2005. Extending the radiocarbon calibration beyond 26,000 years before present using fossil corals. Quaternary Science Reviews 24, 1797–1808.

Cutler, K.B., Gray, S.C., Burr, G.S., Edwards, R.L., Taylor, F.W., Cabioch, G., Beck, J.W., Cheng, H., Moore, J., 2004. Radiocarbon calibration and comparison to 50 kyr BP with paired ^{14}C and ^{230}Th dating of corals from Vanuatu and Papua New Guinea. Radiocarbon 46, 1127–1160.

Fairbanks, R.G., Mortlock, R.A., Chiu, T.-C., Cao, L., Kaplan, A., Guilderson, T.P., Fairbanks, T.W., Bloom, A., Grootes, P.M., Nadeau, M.-J., 2005. Radiocarbon calibration curve spanning 0 to 50,000 years BP based on paired $^{230}Th/^{234}U/^{238}U$ and ^{14}C dates on pristine corals. Quaternary Science Reviews 24, 1781–1796.

Friedrich, M., Kromer, B., Kaiser, K.F., Spurk, M., Hughen, K.A., Johnsen, S.J., 2001. High-resolution climate signals in the Bølling-Allerød Interstadial (Greenland Interstadial 1) as reflected in European tree-ring chronologies compared to marine varves and ice-core records. Quaternary Science Reviews 20, 1223–1232.

Godwin, H., 1962. Radiocarbon dating: fifth international conference. Nature 195, 943.

Hughen, K.A., Southon, J.R., Lehman, S.J., Overpeck, J.T., 2000. Synchronous radiocarbon and climate shifts during the last deglaciation. Science 290, 1951–1954.

Hughen, K.A., Lehman, S.J., Southon, J., Overpeck, J.T., Marchal, O., Herring, C., Turnbull, J., 2004a. ^{14}C activity and global carbon cycle changes over the past 50,000 years. Science 303, 202–207.

Hughen, K.A., Eglinton, T.I., Xu, L., Makou, M., 2004b. Abrupt tropical vegetation response to rapid climate changes. Science 304, 1955–1959.

Johnsen, S.J., Dahl-Jensen, D., Gundestrup, N., Steffensen, J.P., Clausen, H.B., Miller, H., Masson-Delmotte, V., Sveinbjonsdottir, A.E., White, J., 2001. Oxygen isotope and paleotemperature records from six Greenland ice-core stations: Camp Century, Dye-3, GRIP, GISP 2, Renland, and NorthGrip. Journal of Quaternary Science 16, 299–307.

Keigwin, L.D., 2004. Radiocarbon and stable isotope constraints on Last Glacial Maximum and Younger Dryas ventilation in the western North Atlantic. Paleoceanography 19, 15.

Kromer, B., Friedrich, M., Hughen, K.A., Kaiser, F., Remmele, S., Schaub, M., Talamo, S., 2004. Late Glacial ^{14}C ages from a floating, 1270-ring pine chronology. Radiocarbon 46, 1203–1209.

Kump, L.R., 1991. Interpreting carbon-isotope excursions; Strangelove oceans. Geology 19, 299.

Laj, C., Kissel, C., Mazaud, A., Michel, E., Muscheler, R., Beer, J., 2002. Geomagnetic field intensity, North Atlantic Deep Water circulation and atmospheric $\Delta^{14}C$ during the last 50 kyr. Earth and Planetary Science Letters 200, 177–190.

Libby, W.F., 1955. Radiocarbon Dating, second ed. University of Chicago Press, Chicago, IL.

Masarik, J., Beer, J., 1999. Simulation of particle fluxes and cosmogenic nuclide production in the Earth's atmosphere. Journal of Geophysical Research 104, 12,099–12,112.

Meese, D.A., Gow, A.J., Alley, R.B., Zielinski, G.A., Grootes, P.M., Ram, M., Taylor, K.C., Mayewski, P.A., Bolzan, J.F., 1997. The Greenland Ice Sheet Project 2 depth-age scale: methods and results. Journal of Geophysical Research 102, 26,411–26,424.

Peterson, L.C., Haug, G.H., Hughen, K.A., Rohl, U., 2000. Rapid change in the hydrologic cycle of the tropical Atlantc during the last Glacial. Science 290, 1947–1951.

Quay, P., Sonnerup, R., Westby, T., Stutsman, J., McNichol, A., 2003. Changes in the $^{13}C/^{12}C$ of dissolved inorganic carbon in the ocean as a tracer of anthropogenic CO_2 uptake. Global Biogeochemical Cycles 17, 1004.

Reimer, P.J., Baillie, M.G.L., Bard, E., Bayliss, A., Beck, J.W., Bertrand, C.J.H., Blackwell, P.G., Buck, C.E., Burr, G.S., Cutler, K.B., Damon, P.E., Edwards, R.L., Fairbanks, R.G., Friedrich, M., Guilderson, T.P., Hogg, A.G., Hughen, K.A., Kromer, B., McCormac, G., Manning, S., Bronk Ramsey, C., Reimer, R.W., Remmele, S., Southon, J.R., Stuiver, M., Talamo, S., Taylor, F.W., van der Plicht, J., Weyhenmeyer, C.E., 2004. IntCal04 atmospheric radiocarbon age calibration, 26–0 cal kyr BP. Radiocarbon 46, 1029–1058.

Rind, D., Peteet, D., Broecker, W.S., McIntyre, A., Ruddiman, W., 1986. The impact of cold North Atlantic sea surface temperatures on climate: implications for the Younger Dryas cooling (11–10 k). Climate Dynamics 1, 3–33.

Rind, D., Russell, G., Schmidt, G., Sheth, S., Collins, D., deMenocal, P., Teller, J., 2001. Effects of glacial meltwater in the GISS coupled atmosphere-ocean model; 2, A bipolar seesaw in Atlantic Deep Water production. Journal of Geophysical Research 106, 27,355–27,365.

Robinson, L.F., Adkins, J.F., Fernandez, D.P., Wang, S.L., 2004. Past radiocarbon profiles from deep-sea corals in the North Atlantic. EOS Trans. AGU 85(47), Fall Meet. Suppl., S.F., CA.

Schiller, A., Mikolajewicz, U., Voss, R., 1997. The stability of the North Atlantic thermohaline circulation in a coupled ocean-atmosphere general circulation model. Climate Dynamics 13, 325–347.

Severinghaus, J.P., Brook, E.J., 1999. Abrupt climate change at the end of the last Glacial period inferred from trapped air in polar ice. Science 286, 930–934.

Severinghaus, J.P., Sowers, T., Brook, E.J., Alley, R.B., Bender, M.L., 1998. Timing of abrupt climate change at the end of the Younger Dryas interval from thermally fractionated gases in polar ice. Nature 391, 141–147.

Shackleton, N.J., Duplessy, J.C., Arnold, M., Maurice, P., Hall, M.A., Cartlidge, J., 1988. Radiocarbon age of last glacial Pacific deep water. Nature 335, 708–711.

Siegenthaler, U., Oeschger, H., 1987. Biospheric CO_2 emissions during the past 200 years reconstructed by deconvolution of ice core data. Tellus 39B, 141–154.

Sikes, E.L., Samson, C.R., Guilderson, T.P., Howard, W.R., 2000. Old radiocarbon ages in the southwest Pacific Ocean during the last glacial period and deglaciation. Nature 405, 555–559.

Skinner, L.C., Shackleton, N.J., 2004. Rapid transient changes in northeast Atlantic deep water ventilation age across Termination I. Paleoceanography 19, 11.

Southon, J., 2004. A radiocarbon perspective on Greenland ice core chronologies: can we use ice cores for ^{14}C calibration. Radiocarbon 46, 1239–1259.

Spotl, C., Mangini, A., 2002. Stalagmite from the Austrian Alps reveals Dansgaard-Oeschger events during isotope stage 3: implications for the absolute chronology of Greenland ice cores. Earth and Planetary Science Letters 203, 507–518.

Stuiver, M., Polach, H.A., 1977. Discussion; reporting of ^{14}C data. Radiocarbon 19, 355–363.

van der Plicht, J., Beck, J.W., Bard, E., Baillie, M.G.L., Blackwell, P.G., Buck, C.E., Friedrich, M., Guilderson, T.P., Hughen, K.A., Kromer, B., McCormac, F.G., Bronk Ramsey, C., Reimer, P.J., Reimer, R.W., Remmele, S., Richards, D.A., Southon, J.R., Stuiver, M., Weyhenmeyer, C.E., 2004. NotCal04—Comparison/Calibration ^{14}C records 26–50 cal kyr BP. Radiocarbon 46, 1225–1238.

Wang, Y.J., Cheng, H., Edwards, R.L., An, Z.S., Wu, J.Y., Shen, C.-C., Doralee, J.A., 2001. High-resolution absolute-dated late Pleistocene monsoon record from Hulu Cave, China. Science 294, 2345–2348.